PHYSICAL REVIEW VOLUME 86, NUMBER 1 APRIL 1, 1952

Fast Protons from 270-Mev *n–d* Collisions*

J. B. CLADIS, J. HADLEY,† AND W. N. HESS
Radiation Laboratory, Physics Department, University of California, Berkeley, California
(Received December 17, 1951)

The differential cross section for production of high energy protons in *n-d* scattering, using the 270-Mev neutron beam of the 184-in. cyclotron, has been measured at scattering angles between 4° and 58°. For normalization, yields of protons from *n-p* scattering were measured at each scattering angle. In all cases, only protons above a cut-off energy of 200 Mev $\cos^2\Theta$ were accepted by the counter system. In addition, through the use of a magnetic analyzer, energy distributions of the *n-d* protons were measured at 4° and 22.5°. The energy distributions closely resembled, in shape, the energy distributions of *n-p* protons at the same angles, confirming the similarity in nature between collisions of high energy neutrons with free protons and collisions with protons bound in deuterium. Total yield of protons above the cut-off energy is lower for *n-d* than for *n-p* collisions, however, the ratio of the two being about 0.7 at all angles observed. Effects of the exclusion principle, of the internal momentum distribution of the deuteron, and of the difference in average potential energy between the dineutron and the deuteron are discussed as possible causes of the lowering of the *n-d* proton yield below that from *n-p* scattering.

I. INTRODUCTION

COLLISIONS of protons or neutrons with nuclei have generally been thought of in terms of interaction of the incident particle with the whole struck nucleus. According to this point of view, the incident particle may scatter elastically, without changing the internal energy of the nucleus from which it rebounds, or it may enter the nucleus and expend its energy in raising the nuclear temperature, resulting in the eventual expulsion of particles or quanta in random directions. A transition region covering a rather wide energy interval occurs as bombarding energies are increased, however. Above energies of 100 Mev or so, the wavelength or effective size of the bombarding particle is no longer large with respect to separation distances of nucleons. As the energy of the incident particle increases through this region the particle tends more and more to interact with only one nucleon at a time, and the probability for its interaction with any nucleon decreases so that its mean free path within nuclear matter is large. The result of this transition is seen as a basic change in the nature of nucleon-nuclear collisions: with increasing energy, the collision products take on more and more the character of scattered particles from individual nucleon-nucleon collisions. The role of the struck nucleus passes from that of an integral and closely bound system to that of a cloud of separate scattering centers, each moving with a distribution in momentum determined by its interaction with the rest of the nucleus, but otherwise free to act almost independently. One would expect that in the case of very high bombarding energies, emerging particles would be distributed in energy and angle almost as they are in the case of free nucleon-nucleon collisions. Illustrations of this state of affairs may be seen in recent reports on particles ejected from light elements by 240- and 340-Mev protons[1,2] and by 90-Mev neutrons.[3]

The special case of deuterium struck by high energy particles is of particular interest, because of the simplicity of the deuterium nucleus and the relative ease of theoretical treatment of its behavior in collisions. As suggested by the above remarks, one would expect the deuteron to behave very much as two separate particles when it is struck by neutrons of 200- to 300-Mev energy. It should be possible, in fact, to attribute various kinds of emergent particles to collisions of the incident neutron with either one or the other of the deuteron's components. The total scattering cross section can be expressed as a sum of the *n-p* cross section, the *n-n* cross section, and an additional term, probably small, resulting from interference of various kinds.[4–6]

Protons, in particular, resulting from *n-d* collisions, should fall roughly into two groups. A group at low energies would result partly from *n-n* collisions which carry away both neutrons, leaving the proton in about the same state of motion that it was in at the time of collision, and partly from *n-p* collisions in which no charge exchange takes place. The second group, at energies of the order of the bombarding energy and with an angular distribution strongly concentrated in the direction of the incident neutrons, would result from *n-p* collisions with charge exchange. The purpose of the experiments to be described was an investigation of the distribution in angle and energy of the latter proton group, resulting from bombardment of deuterium with a beam of neutrons of about 270-Mev energy. The quantity best determined was the yield of these protons at a number of angles, integrated over energy. The nearness of approach of this quantity to the differential *n-p* scattering yield furnishes a measure

* This work was performed under the auspices of the AEC.
† This report is based on a thesis submitted by J. Hadley in partial satisfaction of the requirements for the degree of Doctor of Philosophy at the University of California.

1 Cladis, Hadley, and Moyer, Phys. Rev. **81**, 649 (1951).
2 G. M. Temmer, Phys. Rev. **83**, 1067 (1951).
3 J. Hadley and H. F. York, Phys. Rev. **80**, 345 (1950).
4 F. de Hoffmann, Phys. Rev. **78**, 216 (1950).
5 G. F. Chew, Phys. Rev. **80**, 196 (1950).
6 R. C. Gluckstern and H. A. Bethe, Phys. Rev. **81**, 761 (1951).

of the accuracy of the concepts stated above regarding the nature of high energy *n-d* collisions; the differences that appear furnish indications of the roles played by effects such as that of the exclusion principle acting on the two neutrons left behind in the collision, and that of the internal momentum distribution of the deuteron. A discussion will be given in the concluding section on such of these factors as appear to influence the measured yield.

II. EXPERIMENTAL PROCEDURE

The experimental procedure chosen consisted of a comparison of the yield of *n-d* protons in the particular energy and angular interval under consideration with the yield of protons from *n-p* scattering in the same interval, measurements of the two quantities being alternated during the course of each experimental run. Most of the final data is expressed in the form of ratios of these quantities, not only because of the convenient nature of such ratios, but also because of the elimination of any effect of varying efficiency of the detecting equipment. The detector efficiency at each angle and energy enters as a factor in the determination of each differential yield, and of course cancels out in the ratio.

The experiment was divided into two main sections, the first being concerned with measurements of differential yields as a function of angle and energy, and the second with measurements of yield as a function of angle, integrated over all energies above a certain cut-off value at each angle. The latter measurements contain no information that could not be derived from the former, but were resorted to through necessity. The length of time necessary to carry out a complete set of measurements, at a number of angles, of differential yields of the former sort would have been prohibitively great.

The necessity of the cut-off energy in the latter part of the experiment arises mainly through the spread in energies of the neutrons comprising the incident beam. In measuring yields from *n-p* scattering in a neutron beam with wide energy spread, it is desired to count just those protons, at each angle, which are produced by neutrons lying within certain energy limits. The energy of scattered protons in *n-p* collisions varies as $E_n \cos^2\Theta$, E_n being the incident neutron energy and Θ the angle of emergence of the proton, measured in the laboratory frame with respect to the direction of the incident neutron. Consequently, for a fixed neutron energy limit, one must vary the energy limit on scattered protons as $\cos^2\Theta$. The cut-off energy chosen in the present experiments was 200 Mev $\cos^2\Theta$, corresponding to a 200-Mev neutron cut off; the same limit was used in the *n-p* scattering experiments of Kelly, Leith, Segrè, and Wiegand.[7] The energy limit used in the measurements of *n-p* yields in the present experiment was chosen to agree with the *n-p* scattering experiments cited above, to permit direct reference to their values of the *n-p* differential scattering cross section. The energy limit used in measurement of yields from *n-d* collisions was also chosen the same for two reasons. First, because the amount of absorber used in setting the cut-off energy affects the efficiency of the counters (nuclear collisions in the absorber material), and it is desirable to keep the counter efficiency the same for both measurements at a given angle, as explained above; and second, because fast protons from high energy *n-d* collisions should approach a $\cos^2\Theta$ energy dependence, and setting a cut-off energy varying as 200-Mev $\cos^2\Theta$ is almost again equivalent to choosing only those protons produced by neutrons of 200-Mev energy or greater.

[7] Kelly, Leith, Segrè, and Wiegand, Phys. Rev. 79, 96 (1950).

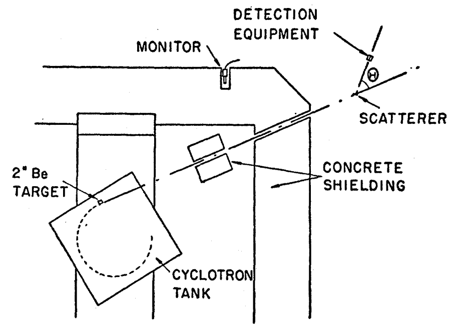

FIG. 1. General experimental arrangement.

The integral measurements were performed with a telescope of counters, arranged so that particles emerging from a scatterer placed in the neutron beam emerging from the 184-in. synchrocyclotron could be observed in any chosen direction. Scattered particles were required to pass through an appropriate thickness of material at each angle, so that only those particles having energy above a fixed lower limit could be counted. During the course of a day's run, measurements of yield at a number of different angles could be made.

Differential measurements were made with a magnetic particle spectrometer, in which particles emerging from the scatterer within a certain small solid angle in a given direction were sorted according to their momentum.

The apparatus was not by itself able to discriminate between protons and deuterons, but theoretical and experimental evidence, which will be discussed later, indicates that practically all of the observed particles were protons, and that no more than a negligible number of elastically scattered deuterons contributed to the observed yields.

Figure 1 shows the over-all experimental arrangement as used in both sections of the experiment.

III. DETAILS OF APPARATUS

A. Neutron Beam

The neutron beam used was produced by placing a 2-inch thick beryllium target in the 350-Mev circulating

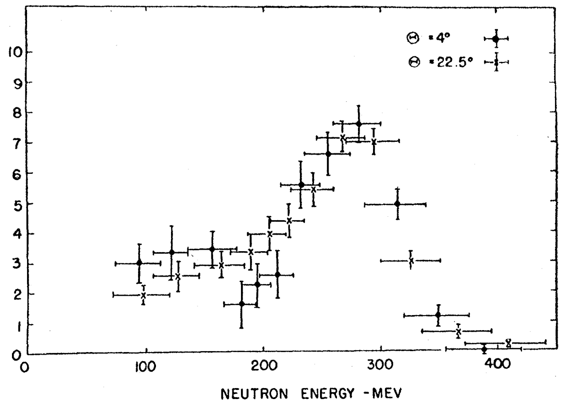

FIG. 2. Energy distribution of neutron beam.

proton beam of the cyclotron. Neutrons emerging in a direction tangent to the path of the proton beam pass through the wall of the cyclotron tank and are collimated in a series of holes through the concrete shielding around the cyclotron before emerging to strike the scatterer.

The distribution in energy of these neutrons has been measured by Kelly *et al.*[7] in connection with *n-p* scattering experiments and can be determined from particle spectrometer results of the present experiment. Figure 2 shows a spectrum derived from the data described in Sec. IV. It is in agreement with those given by other workers.

B. Monitor

In order to compare yields from various scatterers, it is necessary to have some measure of integrated beam intensity. The monitors used for this purpose consisted of boron-trifluoride filled proportional counters placed in holes in the concrete shielding wall. Fast neutrons entering the shielding produce slow neutrons through elastic scattering and through generation of secondary neutrons in collisions with nuclei. The slow neutrons are captured in large numbers by the boron in the counter, and the α-particles produced through the $B^{10}(n,\alpha)Li^7$ reaction are counted. Variation of the neutron beam intensity showed that the counting rate of such a monitor varied in proportion to the counting rate from a scatterer placed directly in the beam.

C. Magnetic Spectrometer

The magnet used to obtain momentum spectra had a pole gap measuring $2\frac{1}{2}$ inches by 12 inches by 30 inches. The maximum field attainable for any considerable length of time was about 14,000 gauss. Electronic current regulation provided a field constant to about $\frac{1}{2}$ of one percent, corresponding to an energy variation of one percent.

In order to define in the magnet, a path having a certain radius of curvature, one must fix three points along the proposed path. Here, the first consisted of the scatterer; the second consisted of a narrow slit at the entrance end of the magnet; and the third was one of a series of G-M tubes located at the exit end of the magnet. At low energies the slit at the entrance end could be defined by a physical gap in some material, but at high energies this system would not be satisfactory. The particle penetration in the gap walls would (1) render the gap width a function of the particle energy, and (2) would degrade the particle energies, causing the energy spectra to be distorted. Because of these effects, small thin-walled proportional counters were used for the second slit. They were made in cylindrical shape, having diameters of $\frac{1}{8}$ inch and $\frac{1}{2}$ inch. The G-M tubes, which located the final points defining the energy channels, were arranged to intercept all protons of energies above about 20 Mev. In this way a complete energy spectrum could be taken in a single measurement. G-M tubes were used in spite of their long dead time because the associated electronic equipment is simpler than for proportional counters. It was found that usable beam intensity was not seriously limited by the effect of dead time.

The pulses originating in the slit counter were fed into the G-M tube amplifiers in such a way that no count from a G-M tube would be registered unless a count from the slit counter arrived within a time interval of about 2 microseconds around the start of the G-M pulse. To eliminate accidental coincidence counts three additional proportional counters were placed within the magnet pole gap, and connected in electronic coincidence with the slit counter. With this system simultaneous pulses in all four proportional counters were necessary to send a "gating" pulse to the G-M tube amplifiers and permit them to register counts. Figure 3 shows the arrangement of the magnet with associated counters.

Determination of the proton energies corresponding to the various magnet channels, at given field settings, was accomplished through use of a light, flexible wire suspended in the pole gap. When a current is passed through the wire, it assumes the same shape as the trajectory of a proton, and the value of $H\rho$, along the wire is given by the ratio of wire tension to wire current.

The spectrometer provided angular resolution of about 1°.

D. Counter Telescopes

The coincidence counter telescopes used in measurements of integrated scattered intensities as a function of angle, consisted of a series of three or sometimes four particle counters fixed with their centers along a straight line passing through the scatterer. The counter system was capable of rotating as a whole about the scatterer. Copper absorbers of varying thickness were placed between the next to last and last counters to fix the lower limit of proton energies that would be accepted by the telescope at the desired value of 200 Mev$\times\cos^2\Theta$.

Part of the experimental data was obtained using proportional counters in the telescope. It was later found that advantage could be taken of the shorter coincidence resolving time and dead time of anthracene scintillation counters to permit the use of a more intense neutron beam without difficulties from accidental coincidences and loss of counter efficiency through dead time. Thus data could be accumulated at a somewhat faster rate, and the proportional counters were accordingly replaced by scintillation counters.

Angular resolution obtained with the counter telescope was about 3°.

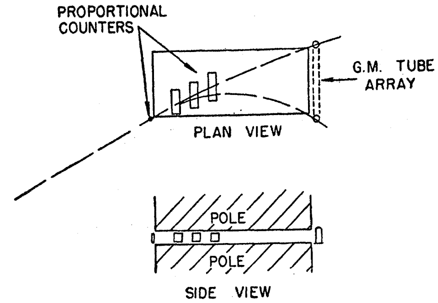

FIG. 3. Schematic diagram of spectrometer.

E. Scatterers

The scatterers used to determine yields of protons from *n-p* collisions were blocks of carbon and polyethylene (CH_2), the hydrogen yield being obtained by taking the carbon-polyethylene difference. Yields from *n-d* collisions were obtained through the use of water and of heavy water scatterers, a subtraction eliminating the oxygen effect and giving the difference in D_2 and H_2 yields. The water and heavy water were held in thin-walled containers, a third identical container being left empty for use as a blank. The scatterers were made taller vertically and narrower horizontally than the neutron beam so that the amount of material in the beam was well known and reproducible. The scatterer thicknesses were chosen so that protons of a given energy suffered equal energy loss in passing through the various scatterers.

IV. REDUCTION OF DATA

A. General Treatment of Data

The yield from each scatterer, normalized to yield per incident neutron through division by appropriate monitor values, will be denoted by symbols in brackets: [H_2O], [D_2O], [CH_2], [C], [B], and [K], where B represents the background yield with no scatterer in place, and K represents the yield with the empty can in place.

To obtain actual yield per mole from each scatterer, we must subtract the background and then divide by the number of moles of scatterer intercepted by the beam, e.g.,

$$\mathrm{CH_2}=\frac{1}{n(\mathrm{CH_2})}([\mathrm{CH_2}]-[B]).$$

The following subtraction then gives the yield per mole resulting from H_2,

$$\mathrm{H_2}=\mathrm{CH_2}-\mathrm{C}=\frac{1}{n(\mathrm{CH_2})}[\mathrm{CH_2}]-\frac{1}{n(\mathrm{C})}[\mathrm{C}]-\frac{n(\mathrm{C})-n(\mathrm{CH_2})}{n(\mathrm{C})n(\mathrm{CH_2})}[B].$$

Similarly,

$$\mathrm{H_2}-\mathrm{D_2}=\frac{1}{n(\mathrm{H_2O})}[\mathrm{H_2O}]-\frac{1}{n(\mathrm{D_2O})}[\mathrm{D_2O}]-\frac{n(\mathrm{D_2O})-n(\mathrm{H_2O})}{n(\mathrm{D_2O})n(\mathrm{H_2O})}[K],$$

and to obtain the deuterium yield,

$$\mathrm{D_2}=\mathrm{H_2}-(\mathrm{H_2}-\mathrm{D_2}).$$

The results of the integral measurements made with the counter telescope are always to be expressed in terms of the quantity (D/H), which may be thought of as the ratio of the fast proton component of the *n-d* cross section to the *n-p* scattering cross section,

$$\frac{\mathrm{D}}{\mathrm{H}}=1-\frac{\mathrm{H_2}-\mathrm{D_2}}{\mathrm{H_2}}=\frac{d\sigma_{n-d(p)}/d\Omega}{d\sigma_{n-p}/d\Omega}.$$

The results of measurements made with the magnet are probably most significant when expressed in terms of the relative quantities D_2 or H_2, so that the actual shapes of spectra are shown. The yield measured in each energy channel must be divided by the counting efficiency of that channel to give proper relative yields.

B. Energy Intervals Accepted by Magnet Channels

Each channel of the magnet accepted protons within an energy interval given by a bell-shaped curve whose form could be derived by a folding process combining the energy uncertainties introduced by each of the three slits. Additional spread in the acceptance interval of each channel was caused by the thickness of the scatterer, and a function describing this was combined with the acceptance function of the magnet channels proper. The energies at half-height of the resulting efficiency curve were taken as the upper and lower limits of the energy interval to which the data from each channel refers, and will be indicated in the presentation of the data. Energy intervals corresponding to the scatterer thickness were obtained from the range-energy curves of Aron, Hoffman, and Williams.[8]

[8] Aron, Hoffman, and Williams, Atomic Energy Commission Unclassified Document No. 663 (1949).

C. Efficiencies for Magnet Channels

The efficiencies of the various magnet channels depended primarily on the width of the G-M tubes. The energy intervals corresponding to these widths were determined from the data obtained from flexible wire calibrations of the magnet.

The effective energy interval of each channel varied with the position in the scatterer of the particular volume element where the protons were produced. Therefore, the effective energy intervals were averaged over the scatterer thickness to obtain the relative channel efficiency for a given scatterer. This was done and the effect of the scatterer was found to be quite small but was included in the efficiencies used.

D. Data obtained with Magnet

Data obtained from magnet runs at scattering angles of 4° and 22.5° are presented in Figs. 4 and 5, which show spectral distributions of yields from hydrogen and from deuterium. The vertical scale of each figure is arbitrary and the scale of Fig. 4 bears no relation to that of Fig. 5. The relative heights of the deuterium and hydrogen spectra in each figure do represent actual relative yields, however. The standard deviation resulting from counting statistics and energy interval pertaining to each point is indicated.

Since the scattered particles from *n-p* collisions have energies that are uniquely determined by the energies of the incident neutrons, it is possible to determine the energy spectrum of a neutron source through a measurement of the energy spectrum from *n-p* scattering at a given angle. In order to carry out such a determination one must have some knowledge of the form of the differential *n-p* scattering cross section as a function of energy at the particular scattering angle used. Figure 6 shows a curve representing this cross section for 8° and 45° scattering angles in the center-of-mass system, as a function of energy. Angles of 8° and 45° in the center-of-mass system correspond nonrelativistically to *n-p* scattering angles of 4° and 22.5° in the laboratory system. Figure 6 was obtained by drawing smooth curves through experimental values of the *n-p* cross section as obtained by various groups.[9] Figure 2 shows energy spectra obtained from the 4° and 22.5° data through division by cross-section values obtained from Fig. 6 and application of the following additional factors. The cross sections given in Fig. 6 refer to unit solid angle in the center-of-mass system, whereas the solid angle referred to in the course of the experiment was constant in the laboratory system. Consequently the variation of center-of-mass solid angle corresponding to a fixed laboratory solid angle must be determined through the relation

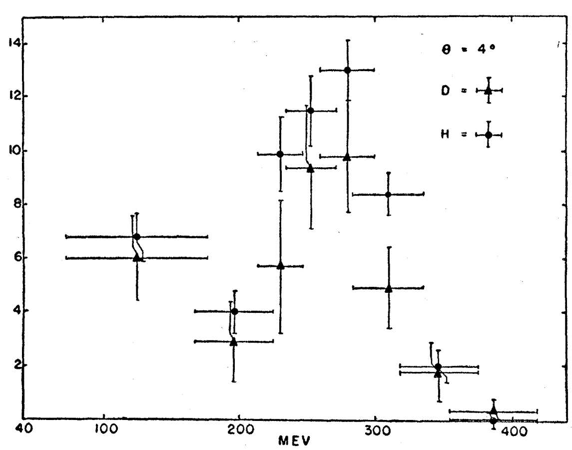

FIG. 4. H and D spectra at 4°.

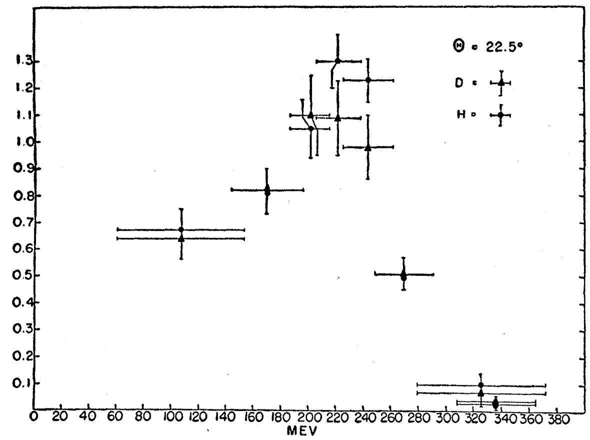

FIG. 5. H and D spectra at 22.5°.

$$d\Omega_{\text{c.m.}}/d\Omega_{\text{lab}}=2(1+\gamma)\cos\Theta/[\cos^2\Theta+\tfrac{1}{2}(1+\gamma)\sin^2\Theta]^2,$$

where Θ = laboratory scattering angle, and $\gamma=1+$neutron energy$/mc^2$.

The second correction factor to be applied arises through the nonlinear relation between neutron and scattered proton energies, causing a variation in neutron energy interval corresponding to unit proton energy interval

$$T_p=\frac{T_n\cos^2\Theta}{1+(T_n/2mc^2)\sin^2\Theta}$$

$$\frac{dT_p}{dT_n}=\frac{\cos^2\Theta}{[1+(T_n/2mc^2)\sin^2\Theta]^2}=\frac{\cos^2\Theta}{[\cos^2\Theta+\tfrac{1}{2}(1+\gamma)\sin^2\Theta]^2}$$

T_n and T_p being the kinetic energies of the incident neutron and scattered proton. The distribution of scattered protons is then related to the distribution of incident neutrons as,

$$\frac{dN_p}{dT_p d\Omega_{\text{lab}}}\propto\frac{dN_n}{dT_n}\cdot\frac{dT_n}{dT_p}\cdot\frac{d\sigma}{d\Omega_{\text{c.m.}}}\cdot\frac{d\Omega_{\text{c.m.}}}{d\Omega_{\text{lab}}},$$

[9] See Hildebrand, Hicks, and Harker, University of California Radiation Laboratory Report No. 1305 (1951); Kelly *et al.*, reference 7; and E. M. Baldwin, Phys. Rev. **83**, 495 (1951) for cross-section values and further references.

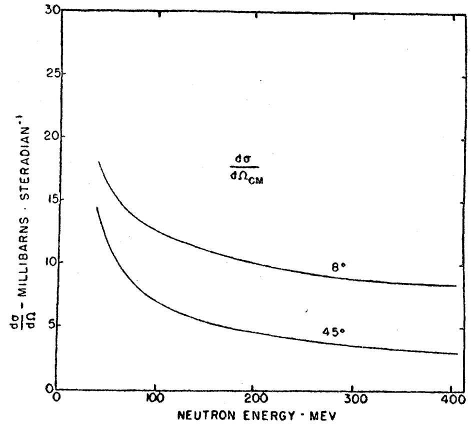

FIG. 6. Values of $d\sigma/d\Omega_{c.m.}$ used in derivation of neutron beam energy spectrum.

or

$$\frac{dN_n}{dT_n} \propto \frac{dN_p}{dT_p d\Omega_{lab}} \cdot \frac{dT_p}{dT_n} \cdot \frac{d\Omega_{lab}}{d\Omega_{c.m.}} \Big/ \frac{d\sigma}{d\Omega_{c.m.}}$$

$$= \frac{dN_p}{dT_p d\Omega_{lab}} \cdot \frac{\cos\Theta}{2(1+\gamma)} \Big/ \frac{d\sigma}{d\Omega_{c.m.}}.$$

E. Considerations on Presence of Scattered Deuterons

Up to this point the scattered particles have been referred to as protons. There was, however, no provision made for excluding other particles, and it would seem important to try to form an estimate of the number and spectrum of deuterons that might be present among particles emerging from n-d collisions.

First, let us refer to the spectra presented in Figs. 4 and 5. The horizontal scales are labeled in terms of proton energies for convenience, but it must be remembered that the actual sorting is according to momentum rather than energy, as each channel represents a certain fixed value of $H\rho$, or momentum, for particles entering it. In the nonrelativistic limit, which will be a sufficiently close approximation for the time being, protons of a given energy, E, will have the same momentum as deuterons of energy $\frac{1}{2}E$. Consequently, if the energy scale of the figures is divided by a factor of 2, an energy scale appropriate to deuterons will result. It is shown in Figs. 4 and 5 that essentially no particles were counted with momenta corresponding to protons of energy greater than about 350 Mev $\cos^2\Theta$, or to deuterons of energy greater than about 175 Mev $\cos^2\Theta$.

The relation between incident neutron energy and elastically scattered deuteron energy is given by

$$E_d = (8/9)E_n \cos^2\Theta$$

setting an upper limit of $(9/8)\times 175 \cong 200$ Mev on the energy of neutrons producing an appreciable number of deuterons through n-d scattering at angles of 4° and 22.5°. More evidence on this point can be adduced from the data presented in Fig. 7. This figure shows spectra obtained in two different ways from D_2O at an angle of 22.5°. The upper set of points represents a spectrum taken in the normal way, while the lower set represents data taken with a carbon absorber of thickness 24 g cm^{-2} placed between the scatterer and magnet. If the curve for no absorber represented only protons, one would expect its form to be preserved when the carbon absorber was used, as correction for proton energy loss in the carbon was made. No deuterons of energy less than 240 Mev can penetrate a carbon thickness of 24 g cm^{-2}, however, so that any deuterons contributing to the spectrum obtained from D_2O without absorber should not be present in the spectrum taken with absorber. It is seen that the two curves lie roughly parallel at proton energies greater than 225 Mev, but that a sharp break in the lower curve occurs at that point. It is felt that this break, at a deuteron energy of $225/2 = 113$ Mev, marks the upper limit of the spectrum of deuterons present. The corresponding neutron energy is

$$E_n = 9\times 113/8 \cos^2 22.5° \cong 150 \text{ Mev}.$$

The almost constant difference between the two curves at energies above the break is felt to represent attenuation in the carbon absorber because of nuclear scattering and inelastic processes. The attenuation factor is about 1.6 ± 0.3, which would correspond to a cross section of 0.33 ± 0.13 barn per carbon nucleus for removal of scattered protons. This value is certainly within reason.

Neutrons of energy 150 Mev and lower seem to produce deuterons at 22.5° from heavy water; we have no information specifically as to whether the source is in the oxygen or in the deuterium. Thus the figure of 150 Mev represents only an upper limit for production in deuterium. It may be that no appreciable number of deuterons is scattered at 22.5° in n-d collisions by neutrons down to a considerably lower energy.

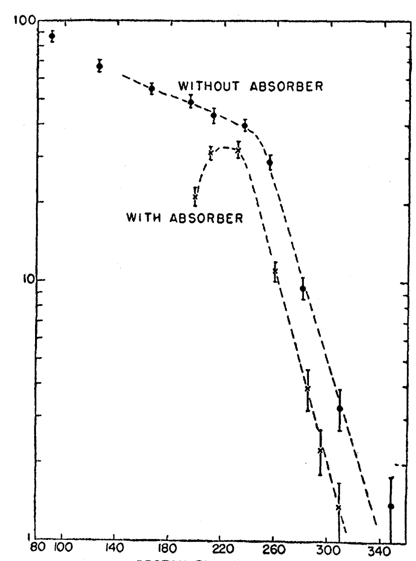

FIG. 7. Effect of carbon absorber on particles from D_2O at 22.5°.

TABLE I. Data from counter telescope runs. Scatterers A: 2.26 g cm^{-2} C equivalent; Scatterers B: 4.02 g cm^{-2} C equivalent.

	Cut-off energy Mev		D/H values from various runs Proportional counters	Scintillation counters			
Θ	A	B	B	A	A	B	Average D/H
4°	195–205	192–209		0.774±0.046		0.704±0.024	0.719±0.201
9°	195–205	191–209	0.670±0.058	0.701±0.066			0.682±0.044
15°	195–205	190–209	0.708±0.063	0.800±0.065			0.752±0.045
22.5°	194–206	189–210	0.697±0.069	0.750±0.086			0.715±0.052
30°	193–207	187–213	0.755±0.108		0.828±0.091	0.926±0.126	0.827±0.061
35°	191–209			0.806±0.113			0.806±0.113
45°	185–215	173–227	0.772±0.128		0.465±0.150		0.643±0.097
55°	169–232			0.513±0.219	0.627±0.142		0.593±0.120
58°	158–243				0.705±0.100		0.705±0.100

Theoretical analysis of n-d elastic scattering[10,11] predicts a weak maximum for deuterons projected forward (pick-up process), and a gradual decrease of cross section with deuteron angle out to well past 60°. This general form is characteristic, regardless of the particular interaction potential used. Consequently, the upper limit of 200 Mev for neutrons producing an appreciable number of scattered deuterons at 4° and 22.5° should hold good for all angles examined in this experiment, the maximum angle at which data was taken being 58°. This fact will be of interest in the next section.

F. Data Obtained with Counter Telescope

Data obtained with the counter telescope was treated in the manner outlined in Sec. IV-A to give values of D/H.

Two separate sets of scatterers were used, one set fairly thin to provide low energy loss by scattered particles in traversing the scatterers, and another set thicker to provide a large quantity of scattering material. The former were used at wide angles, where scattered energies are low, and the latter at small angles, where scattered energies are high and energy loss in the scatterers is of relatively little importance. Particles originating at various depths in the scatterers of course traversed different amounts of material on their way out; the 200 $\cos^2\Theta$ Mev cut-off energy applied only to particles originating in the central plane of the scatterer. As a result the real cutoff took the form of a linear variation in efficiency from 0 to 1 over an energy interval, determined by the scatterer thickness, whose center lay at 200 $\cos^2\Theta$ Mev. Values of lower and upper limits of the cut-off energy interval are tabulated in Table I for both sets of scatterers.

Table I also sets forth values of D/H obtained with each combination of counter type and scatterer size used, together with average values at each angle, which are shown graphically in Fig. 8. Agreement between various sets of data is shown to be good.

Errors tabulated here, as well as with the magnet data, are standard deviations derived from numbers of counts obtained. It is felt that these quantities give a good indication of accuracy of the data, as they are considerably larger than estimated errors likely to have been introduced from other sources.

The absorbers used to provide a proton energy cutoff of 200 $\cos^2\Theta$ Mev also provided a lower energy limit for deuterons accepted, which correspond at each angle to deuterons scattered by neutrons of energy 300 Mev. Since evidence presented in the previous section indicates an upper limit of 200 Mev on neutrons producing a countable number of deuterons at any angle, it is felt safe to assume that the data obtained with the counter telescope refers to scattered protons only.

The integrated D/H value obtained at 22.5° is about 0.7. Comparison with the spectra plotted in Fig. 5 shows that in order to secure agreement, one might assume that part of the D_2 curve results from scattered deuterons. According to this view, and as suggested by the spectra of Fig. 7, one would lower the portion of the D_2 curve lying below 225 Mev by an amount increasing with decreasing energy. The result of such an operation, giving a curve purporting to represent protons alone, might well bring the shape of the D_2 spectrum into close agreement with the shape of the H_2 spectrum. Similar considerations apply to the spectra of Fig. 4.

V. INTERPRETATION OF RESULTS

The experimental results may be described in terms of two main features: first, that the energy spectrum of the fast protons produced at small angles in n-d collisions is a fairly close reproduction, in form, of the energy spectrum of the incident neutrons; and second, that the yield of all protons, of energy greater than 200 $\cos^2\Theta$ Mev, from n-d collisions, bears at each scattering angle the ratio of about 0.7 to the yield of protons, greater than the same cut-off energy, from n-p collisions.

Owing to the wide distribution of incident neutron energies, the first of these features serves merely as a somewhat qualitative demonstration of the similarity of high energy protons from n-d scattering to the protons from n-p scattering. If a more nearly monochromatic neutron beam could be obtained, it would seem well worth while to measure spectra from n-d scattering

[10] G. F. Chew, Phys. Rev. **74**, 809 (1948).

[11] Ta-You Wu and J. Ashkin, Phys. Rev. **73**, 986 (1948).

at wide angles, in order to get information on the effects of the momentum distribution of the deuteron and of the interaction between the two neutrons that are left when a proton is expelled from an *n-d* collision. The breadth of the present neutron spectrum effectively washes out the detailed features of the expelled proton spectrum, and makes the derivation of any information on the above effects quite undependable. For this reason, and also because of the small number of protons produced at wide angles and consequent difficulty in accumulating good statistics, it was not thought worth while to attempt further spectral measurement at present.

The most interesting feature of the data seems to lie in the distribution in angle of the D/H values obtained with the counter telescope. If the proton bound in a deuteron behaved exactly as a free proton in scattering neutrons, one would expect D/H to have the value 1 at all angles. It will be of interest to examine the various perturbing factors which may be the cause of the low value obtained for D/H.

One of the most evident of these factors is the necessity for satisfaction of the Pauli exclusion principle, which should affect the yield of protons in the forward direction. When a fast proton emerges from an *n-d* collision in a direction close to that of the incident neutron, the two residual neutrons must be in a state of low relative momentum. There is a high probability in such a case for the two neutrons to be left in an *S*-state of angular momentum, which will only be possible in the case of antiparallel spins. The consequence is a depression of proton yields at small angles. A different effect must be found which will tend to lower proton yields at wide angles.

Effects which have been proposed as possible causes of the low D/H rate at wide angles are the following: The internal momentum distribution of the deuteron causes, at wide angles, a spread in emerging proton energies, with resultant net displacement of some protons to energies below the cutoff and consequent reduction in measured yield. A second effect of the deuteron's momentum distribution would be of importance if the differential *n-p* cross section, averaged over the motion of the proton in the deuteron, were different from the cross section referring to a stationary proton.

Finally, one might expect that the energy loss involved in converting the deuteron plus neutron system into a dineutron plus proton system would cause the energy of *n-d* protons to be lower than the energy of *n-p* protons at the same angle. The result of this energy shift would be a displacement of part of the proton spectrum below the cut-off energy, with resultant loss in apparent *n-d* yield and lowering of the observed D/H ratio.

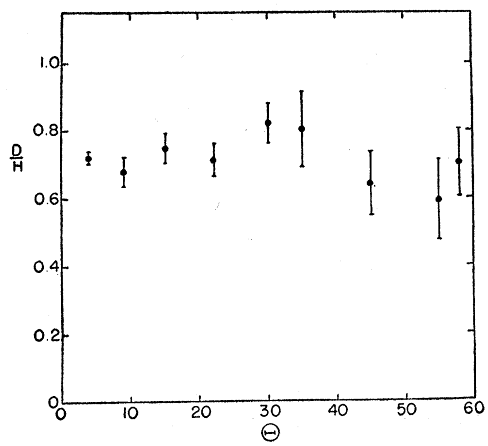

FIG. 8. D/H as a function of angle.

Professor G. F. Chew has supplied us with the results of some calculations on this subject, made in connection with a forthcoming paper on scattering by light nuclei.[12] He finds that the final effect mentioned above, together with the effect of the exclusion principle, gives a D/H ratio close to that observed, and that the form of the D/H curve indicates a very large probability of spin flip in charge-exchange *n-p* collisions. He also finds confirmation in the data for the assumption that the triplet-odd *p-p* force is not attractive.

VI. ACKNOWLEDGMENTS

The authors wish to express their appreciation to the many people who have been of great assistance in the completion of this experiment, and especially to the following: Dr. B. J. Moyer, whose encouragement and suggestions have been of the greatest aid; Dr. G. F. Chew, who suggested the experiment and who has taken an active interest in its interpretation; Dr. Walter Crandall, who worked with the author throughout various preliminary investigations; Dr. Robert Jastrow and Dr. Peter Wolff, who have furnished very helpful discussions regarding interpretation of the experiment; Mr. Boris Ragent, who collaborated in the planning of the spectrometer; Dr. Robert Richardson and Mr. William Ball, who assisted greatly through the loan of scintillation counting equipment; Mr. Hugh Farnsworth and the electronics group under his direction, who designed and maintained the electronics equipment used; and to the crew of the 184-in. cyclotron for their consistent cooperation.

[12] G. F. Chew and G. Placzek (to be published).